

TWO ELLIPTIC HEIGHT MODELS WITH FACTORIZED DOMAIN WALL PARTITION FUNCTIONS

O FODA, M WHEELER AND M ZUPARIC

ABSTRACT. We obtain factorized domain wall partition functions in two elliptic height models: **1.** A Felderhof-type model, which is new, and **2.** A Perk-Schultz-type $gl(1|1)$ model of Deguchi and Martin.

0. INTRODUCTION

0.1. Factorization in trigonometric vertex models. In [1], we obtained factorized domain wall partition functions (DWPF's)¹ in two series of trigonometric vertex models: **1.** The N -state Deguchi-Akutsu models, for $N \in \{2, 3, 4\}$ (and conjectured the result for $N \geq 5$), and **2.** The $gl(r+1|s+1)$ Perk-Schultz models, $\{r, s\} \in \mathbb{N}$ (where given the symmetries of these models, the result is independent of r and s).

0.2. Asymmetry. These models were characterized by an asymmetry of the vertex weights under conjugation of state variables. For example, in the Deguchi-Akutsu model, with state variables $\sigma \in \{1, \dots, N\}$, the vertex weights are non-invariant under the conjugation $\sigma \rightarrow (N - \sigma + 1)$. In the Perk-Schultz models, a similar property holds. Since one can trace the factorization of the DWPF's obtained in [1] to this asymmetry, it is natural to look for height models² with the same property.

0.3. Factorization in elliptic height models. In this work we consider height models, where the state variables are heights, that live on the corners of the faces of a square lattice. A weight is assigned to each face. The weights are elliptic functions of the corresponding rapidities, external fields (if any) and height variables. As in [1], the models in this work are characterized by an asymmetry of the weights, in the sense that the weights of certain vertices (called line-permuting vertices) have different zeros, which leads to the factorization of the DWPF's.

0.4. Summary of results. We obtain factorized DWPF's for two elliptic height models: **1.** A Felderhof-type model, which (to the best of our knowledge) is new, and **2.** A Perk-Schultz-type $gl(1|1)$ model of Deguchi and Martin [3]. These are the first examples of DWPF's for elliptic and/or height models.

0.5. Outline of paper. In Section 1, we collect a number of basic definitions related to elliptic height models to make the paper reasonably self-contained. In Section 2, we introduce a new Felderhof-type elliptic height model and obtain the corresponding factorized DWPF. In Section 3, we do the same for the $gl(1|1)$ elliptic height model of Deguchi and Martin. Section 4 contains brief remarks. The presentation is elementary in the hope that the paper will be reasonably self-contained.

2000 *Mathematics Subject Classification.* Primary 82B20, 82B23.

Key words and phrases. Elliptic height models. Domain wall boundary conditions.

¹For a review of previous results on the subject, see [2].

²Also known as face or interaction-round-face (IRF) models.

1. HEIGHT MODELS

1.1. Faces and corners. We work on a square lattice, as in Figure 1, with L^2 square faces f_{ij} , where $1 \leq i \leq L$ increases from top to bottom, and $1 \leq j \leq L$ increases from left to right. f_{ij} has four corners that are labelled from top-left clockwise as $\{c_{i,j}, c_{i,j+1}, c_{i+1,j+1}, c_{i+1,j}\}$.

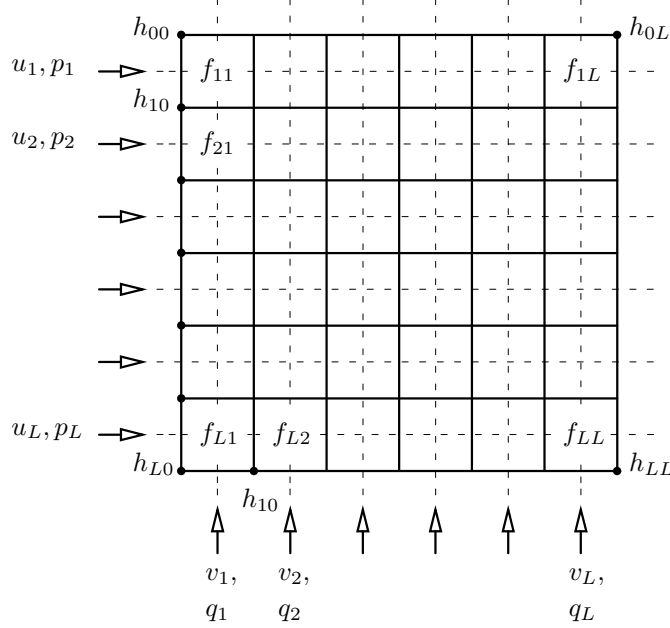


Figure 1. A square lattice with L^2 faces f_{ij} . Rapidities $\{u, v\}$ and external fields $\{p, q\}$ flow along lines that cross the faces. Height variables h_{ij} live on the corners.

1.2. Heights and restrictions. We assign each corner c_{ij} a height variable h_{ij} , $0 \leq i, j \leq L$. In height models such as Baxter's solid-on-solid model [4], the heights are integral (possibly up to an overall shift). In the model of Section 2, the height variables depend linearly on the external fields which are continuous parameters, so they are no longer integral. We define the heights and the restrictions that they obey on a model by model basis in Sections 2 and 3.

1.3. Flow lines, orientations and variables. There are L horizontal and L vertical lines that intersect at the middle points of f_{ij} . They indicate the flow of rapidities and external fields through f_{ij} . We assign the i -th horizontal line an orientation from left to right, a complex rapidity u_i and a complex external field p_i . We assign the j -th vertical line an orientation from bottom to top, a complex rapidity v_j and a complex external field q_j , as in Figure 1.

1.4. Weights and Yang-Baxter equations. We assign each f_{ij} a weight w_{ij} that depends on the height variables on its corners, the difference of the rapidity variables and the two external field variables (if any) flowing through it. The weights satisfy a set of Yang-Baxter equations. The weights and Yang-Baxter equations of the models discussed in this paper are given in Sections 2 and 3.

1.5. Elliptic functions and a theorem. Following the conventions used in [4], Chapter **15**, we consider the elliptic function

$$H(u) = 2q^{1/4} \sin \left(\frac{\pi u}{2I} \right) \prod_{n=1}^{\infty} \left(1 - 2q^{2n} \cos \frac{\pi u}{I} + q^{4n} \right) \left(1 - q^{2n} \right) \quad (1)$$

where $u \in \mathbb{C}$, $q = \exp \left(\frac{-\pi I'}{I} \right)$, $2I$ and $2I'$ (usually called $2K$ and $2K'$) are respectively the (real) width and height of an (upright) rectangle R in the complex u -plane, so that $0 < q < 1$. It is convenient to define

$$[u] = \frac{H(u)}{2q^{1/4}} \quad (2)$$

which is entire and satisfies the quasi-periodicity properties

$$[u + 2I] = -[u] \quad (3)$$

$$[u + 2iI'] = -\frac{1}{q} \exp \left(\frac{-\pi i u}{I} \right) [u] \quad (4)$$

Theorem 1. If $f(u)$ is an entire function that satisfies the quasi-periodicity conditions

$$f(u + 2I) = (-)^L f(u) \quad (5)$$

$$f(u + 2iI') = \left(\frac{-1}{q} \right)^L \exp \left(\frac{-\pi i (Lu - \eta)}{I} \right) f(u) \quad (6)$$

then

$$f(u) = \kappa \left(\prod_{j=1}^{L-1} [u - \zeta_j] \right) \left[u - \eta + \sum_{j=1}^{L-1} \zeta_j \right] \quad (7)$$

where κ and $\zeta_1, \dots, \zeta_{L-1}$ are constants.

Proof. This is a refinement of Theorem **15(c)** of [4], and the proof uses a similar argument. Choose the period rectangle R such that $f(u)$ has no zeros on the boundary ∂R , and integrate $\frac{f'(u)}{f(u)}$ on the anti-clockwise contour ∂R . From the quasi-periodicity conditions it follows that

$$\oint_{\partial R} \frac{f'(u)}{f(u)} du = 2\pi i L \quad (8)$$

Hence the sum of residues of $\frac{f'(u)}{f(u)}$ in R is equal to L , showing $f(u)$ has exactly L zeros in R (counting a zero of order n with multiplicity n). Writing the L zeros as ζ_1, \dots, ζ_L , we define the function $\phi(u) = \prod_{j=1}^L [u - \zeta_j]$. Since $\frac{d}{du} \log(f(u)/\phi(u))$ is doubly periodic (by construction) and holomorphic (also by construction) one has

$$\frac{d}{du} \log \left(\frac{f(u)}{\phi(u)} \right) = \lambda \quad (9)$$

where λ is a constant. Integrating, we obtain $f(u) = \kappa e^{\lambda u} \prod_{j=1}^L [u - \zeta_j]$. Using the quasi-periodicity conditions of $f(u)$, we can, without loss of generality, choose $\lambda = 0$ and $\zeta_L = \eta - \sum_{j=1}^{L-1} \zeta_j$, which concludes the proof.

2. A FELDERHOF-TYPE HEIGHT MODEL

In this section, we introduce an elliptic height model with weights that depend on rapidities, external fields and height variables. In the trigonometric limit, it reduces to the first in a series of models introduced by Deguchi and Akutsu in [5]. In that same limit, and decoupling the dependence on the heights³, it reduces to the trigonometric limit of the elliptic Felderhof vertex model, which is the 2-state Deguchi-Akutsu model [6].

2.1. Notation. Given the rapidities $\{u, v\} \in \mathbb{C}$, external fields $\{p, q\} \in \mathbb{C}$, an upper-left corner height $h \in \mathbb{C}$, $\{\Delta_1, \Delta_2\} \in \{0, 1\}$, $\Delta_3 \in \{0, 1, 2\}$, we use the notation

$$W_{uv} \begin{pmatrix} h & h+q-\Delta_1 \\ h+p-\Delta_2 & h+q+p-\Delta_3 \end{pmatrix} \quad (10)$$

for the weight assigned to the vertex⁴ represented in Figure 2.

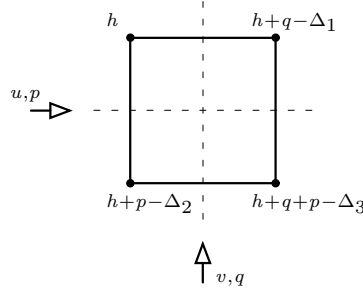


Figure 2. A Felderhof-type face configuration.

2.2. Height restrictions. For $p = q = \frac{1}{2}$, we require that the heights satisfy the same restriction as in Baxter's solid-on-solid model [4], up to a normalization. More precisely,

$$h_{i,j} - h_{i+1,j} = \pm \frac{1}{2}, \quad h_{i,j} - h_{i,j+1} = \pm \frac{1}{2} \quad (11)$$

2.3. The crossing parameter $= \frac{1}{2}$. The vertex weights will be parametrized in terms of the elliptic functions $[u]$. As defined in Equations 1 and 2, $[u]$ depends on the real parameters, I and I' , which are the magnitudes of the half-periods of $[u]$. In the Felderhof-type model discussed in this section, we set $I = 1$ ⁵.

³This can be achieved, for example, by introducing a parameter $\xi \in i\mathbb{R}$, shifting all height variables by ξ (the Yang-Baxter equations remain satisfied), then taking the limit $\xi \rightarrow i\infty$.

⁴In the sequel, we simply say 'vertex' instead of 'face configuration'.

⁵In the limit of zero external fields, that is $p = q = \frac{1}{2}$, this is equivalent to setting the crossing parameter in Baxter's solid-on-solid model to the free fermion point. For details, see [4]

2.4. The weights. In the above notation, the non-zero weights are

$$W_{uv} \begin{pmatrix} h & h+q \\ h+p & h+q+p \end{pmatrix} = a_+(u, v, p, q) = [u - v + p + q] \quad (12)$$

$$W_{uv} \begin{pmatrix} h & h+q-1 \\ h+p-1 & h+q+p-2 \end{pmatrix} = a_-(u, v, p, q) = [v - u + p + q] \quad (13)$$

$$\begin{aligned} W_{uv} \begin{pmatrix} h & h+q-1 \\ h+p & h+q+p-1 \end{pmatrix} &= b_+(u, v, p, q, h) \\ &= \frac{[2h]^{\frac{1}{2}}[2(h+p+q)]^{\frac{1}{2}}}{[2(h+p)]^{\frac{1}{2}}[2(h+q)]^{\frac{1}{2}}} [u - v + q - p] \end{aligned} \quad (14)$$

$$\begin{aligned} W_{uv} \begin{pmatrix} h & h+q \\ h+p-1 & h+q+p-1 \end{pmatrix} &= b_-(u, v, p, q, h) \\ &= \frac{[2h]^{\frac{1}{2}}[2(h+p+q)]^{\frac{1}{2}}}{[2(h+p)]^{\frac{1}{2}}[2(h+q)]^{\frac{1}{2}}} [u - v + p - q] \end{aligned} \quad (15)$$

$$\begin{aligned} W_{uv} \begin{pmatrix} h & h+q \\ h+p & h+q+p-1 \end{pmatrix} &= c_+(u, v, p, q, h) \\ &= \frac{[2p]^{\frac{1}{2}}[2q]^{\frac{1}{2}}}{[2(h+p)]^{\frac{1}{2}}[2(h+q)]^{\frac{1}{2}}} [v - u + p + q + 2h] \end{aligned} \quad (16)$$

$$\begin{aligned} W_{uv} \begin{pmatrix} h & h+q-1 \\ h+p-1 & h+q+p-1 \end{pmatrix} &= c_-(u, v, p, q, h) \\ &= \frac{[2p]^{\frac{1}{2}}[2q]^{\frac{1}{2}}}{[2(h+p)]^{\frac{1}{2}}[2(h+q)]^{\frac{1}{2}}} [u - v + p + q + 2h] \end{aligned} \quad (17)$$

2.5. The Yang-Baxter equations. For rapidities $\{u, v, w\}$, external fields $\{p, q, r\}$, and non-negative integers $\{k, l, m, n, o\}$, the above weights satisfy the Yang-Baxter equations

$$\begin{aligned} &\sum_{j \geq 0} W_{uv} \begin{pmatrix} h & h+q-j \\ h+p-o & h+q+p-n \end{pmatrix} W_{uw} \begin{pmatrix} h+q-j & h+q+r-l \\ h+q+p-n & h+q+r+p-m \end{pmatrix} \\ &\quad \times W_{vw} \begin{pmatrix} h & h+r-k \\ h+q-j & h+r+q-l \end{pmatrix} \\ &= \\ &\sum_{j \geq 0} W_{uv} \begin{pmatrix} h+r-k & h+r+q-l \\ h+r+p-j & h+r+q+p-m \end{pmatrix} W_{uw} \begin{pmatrix} h & h+r-k \\ h+p-o & h+r+p-j \end{pmatrix} \\ &\quad \times W_{vw} \begin{pmatrix} h+p-o & h+p+r-j \\ h+p+q-n & h+p+r+q-m \end{pmatrix} \end{aligned} \quad (18)$$

Proof. This can be proved by direct computation using elliptic function identities, along the same lines as in [4]. For example, when $\{k, l, m, n, o\} = \{0, 1, 1, 1, 1\}$, the Yang-Baxter equation is

$$\begin{aligned}
& \sum_{j=0}^1 W_{uv} \begin{pmatrix} h & h+q-j \\ h+p-1 & h+q+p-1 \end{pmatrix} W_{uw} \begin{pmatrix} h+q-j & h+q+r-1 \\ h+q+p-1 & h+q+r+p-1 \end{pmatrix} \\
& \times W_{vw} \begin{pmatrix} h & h+r \\ h+q-j & h+r+q-1 \end{pmatrix} \\
& = W_{uv} \begin{pmatrix} h+r & h+r+q-1 \\ h+r+p-1 & h+r+q+p-1 \end{pmatrix} W_{uw} \begin{pmatrix} h & h+r \\ h+p-1 & h+r+p-1 \end{pmatrix} \\
& \times W_{vw} \begin{pmatrix} h+p-1 & h+p+r-1 \\ h+p+q-1 & h+p+r+q-1 \end{pmatrix} \tag{19}
\end{aligned}$$

Using the expressions for the weights, we obtain

$$\begin{aligned}
& c_-(u, v, p, q, h) a_+(u, w, p, r) b_-(v, w, q, r, h) \\
& + b_-(u, v, p, q, h) c_-(u, w, p, r, h+q) c_+(v, w, q, r, h) \\
& = c_-(u, v, p, q, h+r) b_-(u, w, p, r, h) a_+(v, w, q, r) \tag{20}
\end{aligned}$$

Writing the weights in terms of elliptic functions, one can eliminate common factors, and the proof of the equation reduces to proving

$$\begin{aligned}
& [u-v+p+q+2h][u-w+p+r][v-w+q-r][2(h+q+r)] \\
& + [u-v+p-q][u-w+p+r+2(h+q)][w-v+q+r+2h][2r] \\
& = [u-v+p+q+2(h+r)][u-w+p-r][v-w+q+r][2(h+q)] \tag{21}
\end{aligned}$$

which proceeds by noting that the ratio of the left-hand-side and right-hand-side is doubly periodic and entire in u , and therefore a constant with respect to u . Setting $u = v - p + q$, the constant is found to be 1.

2.6. Switching off the external fields. Setting $p = q = \frac{1}{2}$ is equivalent to switching off the external fields. This becomes clear by inspection of the vertex weights, which up to normalization become equal to those of Baxter's solid-on-solid model at the free fermion point.

2.7. The external fields tilt the heights. One can think of the external fields $p \neq \frac{1}{2}$ and/or $q \neq \frac{1}{2}$, as effectively *tilting* the heights of the lattice faces that they flow through. This tilt is with respect to the line along which a field flows. This effectively adds to or subtracts from the height differences that are the case in the absence of external fields.

2.8. The c_+ vertex. In discussions of DWBC's and DWPF's, the c_+ vertex, see Figure 3, plays a special role: It is the DWPF for a 1×1 square lattice.

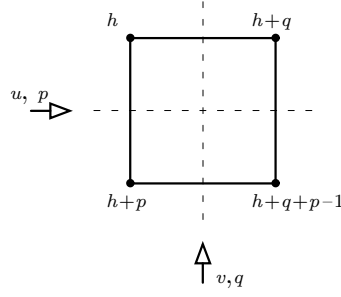


Figure 3. The Felderhof-type c_+ vertex.

2.9. Domain wall boundary conditions (DWBC). We define the DWBC's as an *expanded* c_+ vertex, as in Figure 4: Given the external fields $\{p, q\}$ and starting from $h_{00} = h$ at the top-left corner, the boundary heights change by q_j from left to right along the upper boundary, $p_i - 1$ from top to bottom along the right boundary, $-q_j + 1$ from right to left along the lower boundary, and $-p_i$ from bottom to top along the left boundary.

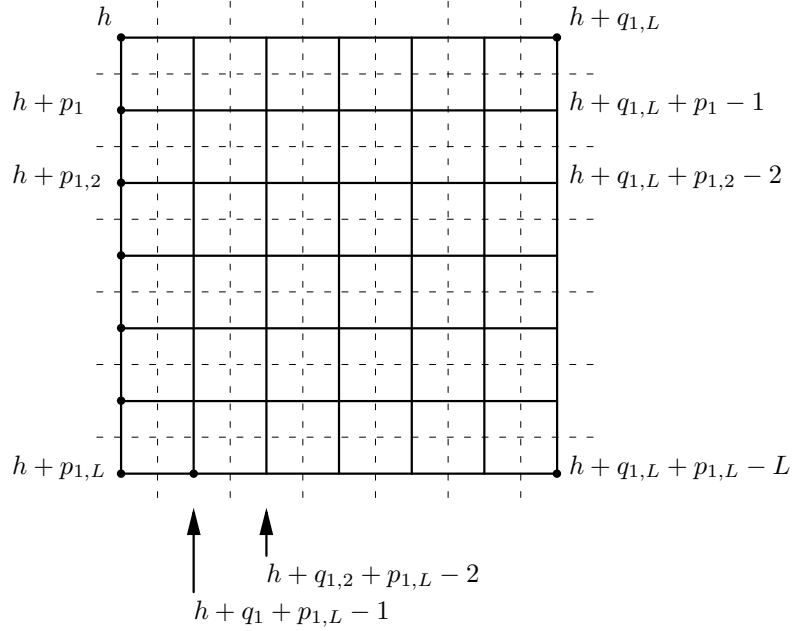


Figure 4. Felderhof-type height domain wall boundary conditions. We use the notation $p_{i,j} = \sum_{k=i}^j p_k$, etc.

2.10. Domain wall partition function (DWPF). The DWPF on an $L \times L$ lattice, $Z_{L \times L}$, is the sum over all weighted configurations that satisfy the DWBC. The weight of each configuration is the product of the weights of the vertices

$$Z_{L \times L} = \sum_{\text{configurations}} \left(\prod_{\text{vertices}} w_{ij} \right) \quad (22)$$

2.11. Line permuting vertices. In proofs of DWPF's two vertices play an important role. These are the a -type vertices which can be used to permute adjacent flow lines.

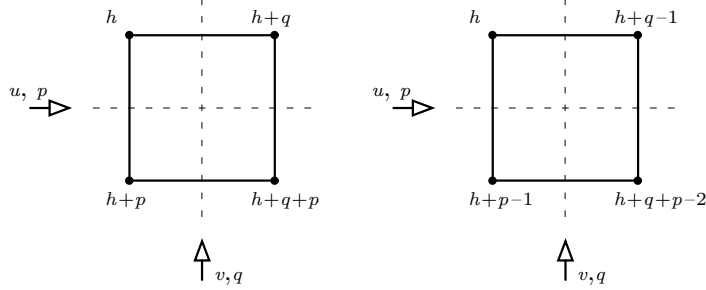


Figure 5. The Felderhof-type line permuting vertices a_+ and a_- .

2.12. Different zeros. The weights of the line permuting vertices, $[u - v + p + q]$ and $[v - u + p + q]$, have different zeros. This is the property that will allow us to obtain the zeros of the DWPF and compute it in factorized form.

2.13. Properties of the partition function. The following four properties determine the partition function uniquely.

2.13.1. Property 1: Quasi-periodicity. The partition function is entire in u_1 and satisfies the quasi-periodicity conditions

$$Z_{L \times L} \left(u_1 + 2, \dots, u_L, \{v\}, \{p\}, \{q\}, h \right) = (-)^L Z_{L \times L} \left(\{u\}, \{v\}, \{p\}, \{q\}, h \right) \quad (23)$$

$$\begin{aligned} & Z_{L \times L} \left(u_1 - \frac{2i \log(\mathbf{q})}{\pi}, \dots, u_L, \{v\}, \{p\}, \{q\}, h \right) = \\ & \frac{(-)^L}{\mathbf{q}^L} \exp \left[-\pi i \left(Lu_1 + (L-2)p_1 - \sum_{j=1}^L (v_j + q_j) - 2h \right) \right] \times \\ & Z_{L \times L} \left(\{u\}, \{v\}, \{p\}, \{q\}, h \right) \end{aligned} \quad (24)$$

Proof. Since the weights are entire functions in the rapidities, it follows that $Z_{L \times L} \left(\{u\}, \{v\}, \{p\}, \{q\}, h \right)$ is an entire function in u_1 . To prove the quasi-periodicity conditions, we write the partition function in the form

$$\begin{aligned} Z_{L \times L} \left(\{u\}, \{v\}, \{p\}, \{q\}, h \right) &= \sum_{n=1}^L P_n \left(u_1, \{v\}, p_1, \{q\}, h \right) \times \\ & Q_n \left(u_2, \dots, u_L, \{v\}, p_2, \dots, p_L, \{q\}, h \right) \end{aligned} \quad (25)$$

where

$$\begin{aligned}
 P_n \left(u_1, \{v\}, p_1, \{q\}, h \right) &= \left(\prod_{j=1}^{n-1} a_+(u_1, v_j, p_1, q_j) \right) c_+ \left(u_1, v_n, p_1, q_n, h + \sum_{k=1}^{n-1} q_k \right) \\
 &\times \left(\prod_{j=n+1}^L b_-(u_1, v_j, p_1, q_j, h + \sum_{k=1}^{j-1} q_k) \right)
 \end{aligned} \tag{26}$$

and $Q_n \left(u_2, \dots, u_L, \{v\}, p_2, \dots, p_L, \{q\}, h \right)$ does not depend on u_1 . Using the expressions for the weights, we have

$$P_n \left(u_1 + 2, \{v\}, p_1, \{q\}, h \right) = (-)^L P_n \left(u_1, \{v\}, p_1, \{q\}, h \right) \tag{27}$$

$$P_n \left(u_1 - \frac{2i \log(\mathbf{q})}{\pi}, \{v\}, p_1, \{q\}, h \right) = \tag{28}$$

$$\frac{(-)^L}{\mathbf{q}^L} \exp \left[-\pi i \left(Lu_1 + (L-2)p_1 - \sum_{j=1}^L (v_j + q_j) - 2h \right) \right] P_n \left(u_1, \{v\}, p_1, \{q\}, h \right)$$

from which the required property follows immediately.

2.13.2. Property 2: Simple zeros. The partition function has simple zeros at $u_1 = u_j - p_1 - p_j$, where $j = 2, \dots, L$.

Proof. We multiply the partition function by $a_+(u_2, u_1, p_2, p_1)$, and use the Yang-Baxter equation to slide the inserted face through the lattice.

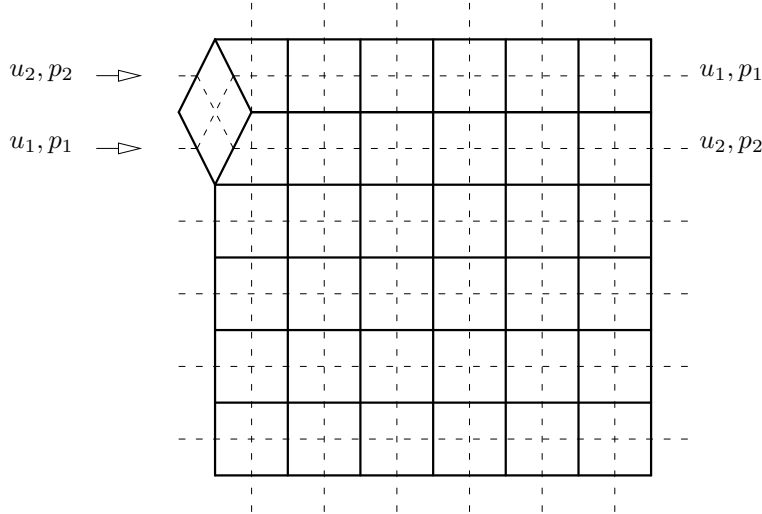


Figure 6. Inserting an a_+ vertex into the left boundary.

It emerges as $a_-(u_2, u_1, p_2, p_1)$, and the order of the first two lattice rows is reversed.

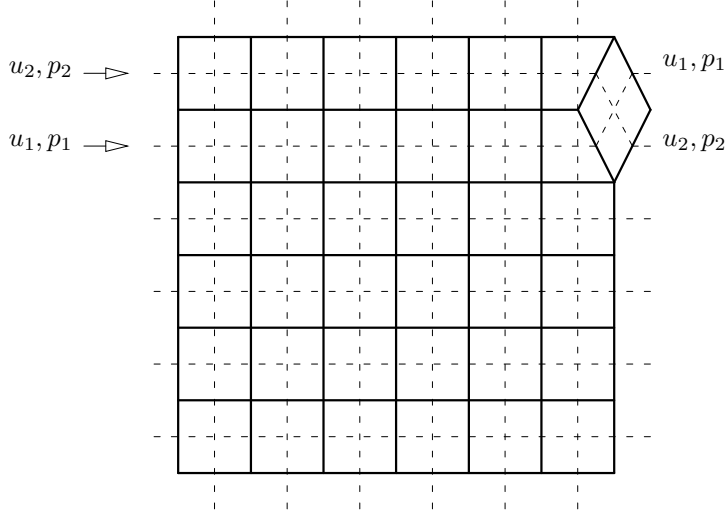


Figure 7. *Extracting an a_- vertex from the right boundary.*

This is equivalent to the equation

$$Z_{L \times L} \left(\{u\}, \{v\}, \{p\}, \{q\}, h \right) = \frac{a_-(u_2, u_1, p_2, p_1)}{a_+(u_2, u_1, p_2, p_1)} \times \quad (29)$$

$$Z_{L \times L} \left(u_2, u_1, \dots, u_L, \{v\}, p_2, p_1, \dots, p_L, \{q\}, h \right)$$

Repeating this procedure on the second and third rows, and so on, we obtain

$$Z_{L \times L} \left(\{u\}, \{v\}, \{p\}, \{q\}, h \right) = \prod_{j=2}^L \left(\frac{a_-(u_j, u_1, p_j, p_1)}{a_+(u_j, u_1, p_j, p_1)} \right) \times \quad (30)$$

$$Z_{L \times L} \left(u_2, \dots, u_L, u_1, \{v\}, p_2, \dots, p_L, p_1, \{q\}, h \right)$$

which has the required simple zeros in the numerator.

2.13.3. Property 3: A recursion relation. The partition function satisfies the recursion relation

$$Z_{L \times L} \left(\{u\}, \{v\}, \{p\}, \{q\}, h \right) \Big|_{u_1=v_1-p_1-q_1} = c_+(v_1 - p_1 - q_1, v_1, p_1, q_1, h) \times$$

$$\left(\prod_{j=2}^L b_+(u_j, v_1, p_j, q_1, h + \sum_{k=1}^{j-1} p_k) b_-(v_1 - p_1 - q_1, v_j, p_1, q_j, h + \sum_{k=1}^{j-1} q_k) \right) \times$$

$$Z_{(L-1) \times (L-1)} \left(u_2, \dots, u_L, v_2, \dots, v_L, p_2, \dots, p_L, q_2, \dots, q_L, h + p_1 + q_1 - 1 \right) \quad (31)$$

Proof. In any lattice configuration in the partition function sum, the top-left corner of the lattice must be $a_+(u_1, v_1, p_1, q_1)$ or $c_+(u_1, v_1, p_1, q_1, h)$. Setting $u_1 = v_1 - p_1 - q_1$ in the partition function sets to zero all configurations with $a_+(u_1, v_1, p_1, q_1)$.

The surviving configurations must have a top-left corner equal to c_+ , which fixes the rest of the top row to b_- , the rest of the first column to b_+ , and the remainder

of the lattice to $Z_{(L-1) \times (L-1)}$. The above recursion follows immediately from these considerations.

2.13.4. *Property 4.* The partition function on a 1×1 lattice is given by

$$Z_{1 \times 1}(u_1, v_1, p_1, q_1, h) = c_+(u_1, v_1, p_1, q_1, h) \quad (32)$$

Proof. This follows from the definition of domain wall boundary conditions.

2.14. **The partition function is uniquely determined.** Assume that $Z_{(n-1) \times (n-1)}$ is uniquely determined by the above four properties, for some $n \geq 2$. From Property 1, Property 2 and Theorem 1.1, we have

$$\begin{aligned} Z_{n \times n} \left(\{u\}, \{v\}, \{p\}, \{q\}, h \right) &= \kappa(u_2, \dots, u_n, \{v\}, \{p\}, \{q\}) \times \\ &\left[\sum_{j=1}^n (v_j - u_j) + \sum_{j=1}^n (p_j + q_j) + 2h \right] \left(\prod_{j=2}^n [u_1 - u_j + p_1 + p_j] \right) \end{aligned} \quad (33)$$

Property 3 fully determines the coefficient κ in terms of $Z_{(n-1) \times (n-1)}$. Finally, since $Z_{1 \times 1}$ is uniquely determined by Property 4, $Z_{n \times n}$ is uniquely determined by the four properties.

2.15. **The domain wall partition function.** The solution to the preceding four properties is given by

$$\begin{aligned} Z_{L \times L} \left(\{u\}, \{v\}, \{p\}, \{q\}, h \right) &= \frac{\prod_{j=1}^L [2p_j]^{\frac{1}{2}} [2q_j]^{\frac{1}{2}}}{[2(h + \sum_{j=1}^L p_j)]^{\frac{1}{2}} [2(h + \sum_{j=1}^L q_j)]^{\frac{1}{2}}} \times \\ &\left[\sum_{j=1}^L (v_j - u_j) + \sum_{j=1}^L (p_j + q_j) + 2h \right] \prod_{1 \leq j < k \leq L} [u_j - u_k + p_j + p_k][v_k - v_j + q_k + q_j] \end{aligned} \quad (34)$$

2.16. **Two choices of DWBC's.** There are two possible choices of DWBC's. One corresponds to an *expanded* c_+ , as in this work, and one to an 'expanded' c_- vertex. The DWPF depends on the choice. The two expressions coincide for vanishing external fields, that is $p_i = q_j = \frac{1}{2}$, and appropriate choices of the boundary height variables.

3. A PERK-SCHULTZ-TYPE $gl(1|1)$ HEIGHT MODEL

In [3], Deguchi and Martin introduced elliptic height versions of the $gl(r+1|s+1)$ trigonometric vertex models. In the following, we define DWBC's and compute the DWPF in the $gl(1|1)$ case. Since the analysis in this Section follows almost verbatim that of Section 2, we will be brief and give just enough details where the two models differ.

3.1. Notation, heights and restrictions. In this model, there are two square lattices. A *physical* $L \times L$ lattice that the heights live on, and a *target* $\mathbb{Z} \times \mathbb{Z}$ lattice that the heights take values in. The target lattice is spanned by the unit vectors \hat{e}_μ , $\mu \in \{-1, +1\}$, thus the height variables are 2-component vectors $\{h_\mu, h_\nu\}$. Heights on adjacent physical lattice corners are restricted to take values in adjacent points on the target lattice. Height differences along \hat{e}_{-1} and \hat{e}_{+1} lead to different vertex weights. To each height vector $h = \{h_\mu, h_\nu\}$, we assign a scalar

$$h_{\mu\nu} = h_\mu + h_\nu + \omega_{\mu\nu} \quad (35)$$

where ω is an arbitrary constant antisymmetric complex 2×2 matrix. We use \hat{e}_μ as well as $\hat{e}_{\text{sign}(\mu)}$ to indicate the same unit vector.

3.2. No external fields and the crossing parameter is a variable. Unlike the previous Felderhof-type model, the Perk-Schultz-type model in this Section has no external fields. The crossing parameter is left as a variable.

3.3. The weights. The non-zero vertex weights are

$$W_{uv} \begin{pmatrix} h & h + \hat{e}_\mu \\ h + \hat{e}_\mu & h + 2\hat{e}_\mu \end{pmatrix} = a_\mu(u, v) = \frac{[1 + \mu(u - v)]}{[1]} \quad (36)$$

$$W_{uv} \begin{pmatrix} h & h + \hat{e}_\nu \\ h + \hat{e}_\mu & h + \hat{e}_\mu + \hat{e}_\nu \end{pmatrix} = b_\mu(u, v) = \frac{[u - v][h_{\mu\nu} - 1]}{[1][h_{\mu\nu}]}, \quad \mu \neq \nu \quad (37)$$

$$W_{uv} \begin{pmatrix} h & h + \hat{e}_\mu \\ h + \hat{e}_\mu & h + \hat{e}_\mu + \hat{e}_\nu \end{pmatrix} = c_\mu(u, v) = \frac{[h_{\mu\nu} - (u - v)]}{[h_{\mu\nu}]}, \quad \mu \neq \nu \quad (38)$$

The variables $h_{\mu\nu}$ on the right hand sides of Equations 37 and 38 are the scalars assigned to the heights at the upper left corners of the corresponding vertices.

3.4. The Yang-Baxter equations. The weights satisfy the following Yang-Baxter equations [3].

$$\begin{aligned} \sum_{g \in \mathbb{Z}^2} W_{u_1 u_2} \begin{pmatrix} b & g \\ a & f \end{pmatrix} W_{u_1 u_3} \begin{pmatrix} g & d \\ f & e \end{pmatrix} W_{u_2 u_3} \begin{pmatrix} b & c \\ g & d \end{pmatrix} = \\ \sum_{g \in \mathbb{Z}^2} W_{u_2 u_3} \begin{pmatrix} a & g \\ f & e \end{pmatrix} W_{u_1 u_3} \begin{pmatrix} b & c \\ a & g \end{pmatrix} W_{u_1 u_2} \begin{pmatrix} c & d \\ g & e \end{pmatrix} \end{aligned} \quad (39)$$

3.5. The c_+ vertex. We take the c_+ vertex to be as in Figure 8.

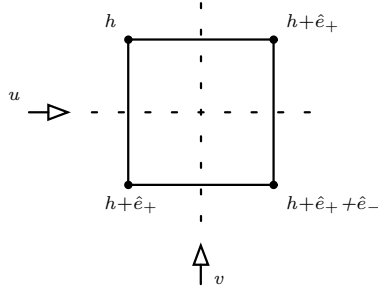


Figure 8. A general face configuration.

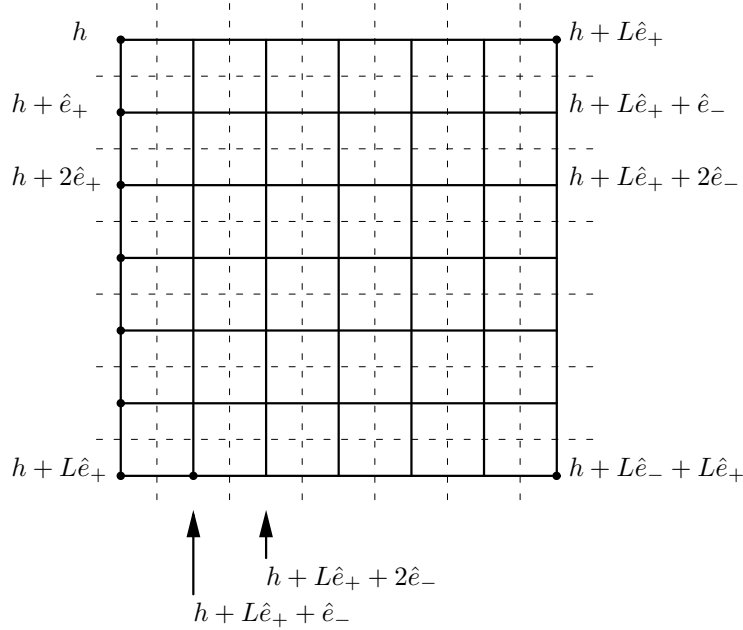


Figure 9. *Perk-Schultz-type height domain wall boundary conditions.*

3.6. The domain wall boundary conditions. We choose the DWBC as in Figure 9. In other words, starting from the lower left corner, all height changes along the left boundary are of type \hat{e}_{+1} , along the upper boundary they are of type \hat{e}_{-1} , along the right boundary they are of type \hat{e}_{+1} , then along the lower boundary they are of type \hat{e}_{-1} .

3.7. The line-permuting vertices. We take the line permuting vertices to be as in Figure 10. Their weights have different zeros leading to a factorization of the DWPF, just as in Section 2.

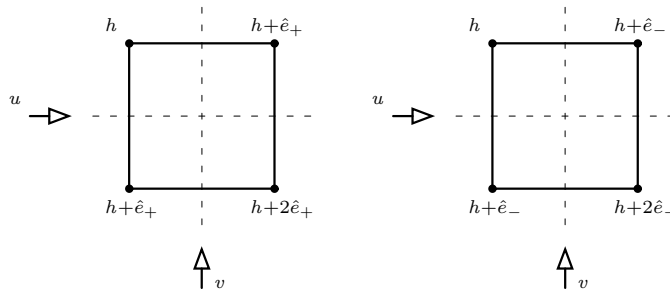


Figure 10. *The Perk-Schultz-type line permuting vertices a_+ and a_- .*

3.8. The DWPF. Having defined the model, the derivation of the corresponding DWPF proceeds precisely in analogy with that in Section 2. Based on the quasi-periodicity properties of the partition function, we propose a factorization in terms of the $[u]$ functions. We obtain the zeros by permuting adjacent flow lines, using the line permuting vertices, obtain a recursion relation the DWPF satisfies and an

initial condition. The DWPF is uniquely determined, and the following expression satisfies all the conditions.

$$Z_{L \times L} = \frac{[h + (L - 1) - \sum_{k=1}^L (u_k - v_k)]}{[h + (L - 1)]} \prod_{1 \leq i < j \leq L} \frac{[1 + u_i - u_j]}{[1]} \frac{[1 - (v_i - v_j)]}{[1]} \quad (40)$$

3.9. On the $gl(r + 1|s + 1)$ height models. The reason we chose the $gl(1|1)$ case is that, given the way that we define DWBC's, the symmetries of the $gl(r + 1|s + 1)$ models are such that only the two state variables variables that we put on the domain wall boundaries end up propagating inside the configurations. This effectively restricts the DWPF to the $gl(1|1)$ model.

4. REMARKS

The point of this work is to give examples of domain wall partition functions in elliptic and/or height models. We restricted our attention to models that are non-invariant under state variable conjugation, which greatly simplified the problem.

Because of the fermionic nature of the models discussed in this paper, there is no interesting applications of their DWPF's to enumerations of alternating sign matrices or related objects that we are aware of.

It is highly likely that all models that are non-invariant under some form of state variable conjugation, that allows factorization, are fermionic (as the Felderhof-type model of Section 2) or contain fermions that play an essential role in the definition of the DWBC's (as the Perk-Schultz-type model of Section 3). As such, these models are unrepresentative of the general case. However, they are non-trivial and we hope that one can learn something by extending our results to compute correlation functions.

ACKNOWLEDGEMENTS

OF would like to thank Professors R J Baxter, T Deguchi and M Jimbo for discussions, and P Bouwknegt, T Guttman and T Miwa for hospitality at ANU, MASCOS and Kyoto University, while this work was in progress. MW and MZ are supported by an Australian Postgraduate Award (APA).

REFERENCES

- [1] O FODA, M WHEELER AND M ZUPARIC, *J Stat Mech* (2007) P10016 [arXiv:0709.4540](#)
- [2] V E KOREPIN AND O I PATU, *XXX spin chain: From Bethe solution to open problems*, [arXiv:cond-mat/0701491](#)
- [3] T DEGUCHI AND P P MARTIN *Int J Mod Phys A* **7**, Suppl. **1A**(1992) 165-196
- [4] R J BAXTER *Exactly solved models*,
- [5] T DEGUCHI AND A AKUTSU, *J Phys Soc of Japan* **62** (1993) 19-35.
- [6] T DEGUCHI AND A AKUTSU, *J Phys Soc of Japan* **60** (1991) 4051-4059.

DEPARTMENT OF MATHEMATICS AND STATISTICS, UNIVERSITY OF MELBOURNE, PARKVILLE, VICTORIA 3010, AUSTRALIA.

E-mail address: foda, mwheeler, mzup@ms.unimelb.edu.au